SCIENCE CHINA Materials ARTICLES

mater.scichina.com link.springer.com

Published online 16 April 2018 | https://doi.org/10.1007/s40843-018-9266-8
Sci China Mater 2018, 61(7): 969–976

A skin-like stretchable colorimetric temperature sensor

Yingzhi Chen[1], Yin Xi[1], Yujie Ke[2], Wenhao Li[1], Yi Long[2], Jingyuan Li[1], Lu-Ning Wang[1,3*] and Xiaohong Zhang[4*]

ABSTRACT **Wearable and stretchable physical sensors that can conformally contact on the surface of organs or skin provide a new opportunity for human-activity monitoring and personal healthcare. Particularly, various attempts have been made in exploiting wearable and conformal sensors for thermal characterization of human skin. In this respect, skin-mounted thermochromic films show great capabilities in body temperature sensing. Thermochromic temperature sensors are attractive because of their easy signal analysis and optical recording, such as color transition and fluorescence emission change upon thermal stimuli. Here, desirable mechanical properties that match epidermis are obtained by physical crosslinking of polydiacetylene (PDA) and transparent elastomeric polydimethylsiloxane (PDMS) networks. The resulting PDA film displayed thermochromic and thermofluorescent transition temperature in the range of 25–85°C, with stretchability up to 300% and a skin-like Young's modulus of ~230 kPa. This easy signal-handling provides excellent references for further design of convenient noninvasive sensing systems.**

Keywords: stretchable, skin-like, thermochromic, thermofluorescent, temperature sensor

INTRODUCTION

Ongoing efforts have been devoted to the development of smart and wearable/implantable devices for ubiquitous computing or personalized medical care [1–5]. A key technical issue in designing such wearable devices is to achieve reasonable stretchability and delightful deformability. It is acknowledged that conventional devices built on the rigid planar, brittle surfaces (e.g., metal and semiconductor wafer) cannot survive undergoing large mechanical deformations because of their high Young's modulus (>10 GPa) with limited stretchability (<5%). Different from them, the main advantages of stretchable systems are associated with their low modulus, light weight, and large deformability without performance failure, and thus enabling close skin contact and conformal lamination onto complex nonplanar surfaces [6,7]. To date, various flexible or stretchable devices have been used in the field of flexible display, and wearable technologies such as health monitoring and soft robotics [8–13]. For instance, high-adhesion stretchable electrodes have been used both for stretchable electrodes and strain sensors to reliably detect electromyography signals and the joint motions [14]. Polymeric microelectrode arrays have been fabricated with high stretchability of 100%, and used for conformally recording the electrocorticography signals from rats in normal and epileptic states [15]. In another example, surface strain redistribution is reported to significantly enhance the sensitivity of fiber-shaped stretchable strain sensors that can be reliably used to monitor the sports activity [16].

Among the various flexible devices, highly stretchable and biocompatible temperature sensors can serve as a comfortable and compliant system towards personal healthcare [6,17–19]. To design these responsive soft material systems, various strategies have been exploited, such as integrating the sensor chips or circuits onto the flexible substrates, or doping the functional materials into the polymer matrix. In one case, a temperature sensor, which was firstly fabricated on a silicon-on-insulator wafer and then transferred to a prestrained elastomeric polydimethylsiloxane (PDMS) substrate, could be stretched and compressed up to 30% [20]. Likewise, a wear-

[1] School of Materials Science and Engineering, University of Science and Technology Beijing, Beijing 100083, China
[2] School of Materials Science and Engineering, Nanyang Technological University, Singapore 639798, Singapore
[3] State Key Laboratory for Advanced Metals and Materials, University of Science and Technology Beijing, Beijing 100083, China
[4] Institute of Functional Nano and Soft Materials (FUNSOM), Soochow University, Suzhou 215123, China
* Corresponding authors (emails: luning.wang@ustb.edu.cn (Wang LN); xiaohong_zhang@suda.edu.cn (Zhang X))

© Science China Press and Springer-Verlag GmbH Germany 2018

able sensor consisting of flexible circuits and materials was designed to measure the brain temperature [21]. In another report, a Ni microparticle-filled binary polymer composite was fabricated as a flexible wireless sensor to monitor human body temperature [22]. A similar methodology was also seen with the use of PDMS and polyimide (PI) to disperse graphite for flexible temperature sensor arrays [23]. However, the sensation information mainly depends on electric detector and electricity input, which is not directly conveyed. For a convenient and comfortable sensor, it is highly desirable for the signal readout to be directly visualized by the naked eye in a simplified operation condition [24–26].

Thermochromic materials can provide visual response to thermal stimulus. The change in color, absorption and luminescence can be directly visualized by the naked eye and captured by the optical detectors. In this aspect, polydiacetylene (PDA) appears to be a favorable choice [27–31]. PDA was selected as the thermo-responsive element for this platform owing to their responsive color transition (blue-to-red) and fluorescence change (non-to-red) when subjected to thermal stimulus. The blue-to-red colorimetric transition is directly visible to the naked eyes. Undoubtedly, a good combination of this characteristic and high stretchability facilitates detection easily, and more importantly, enables safe and compliant human interaction. In this respect, PDMS is still an excellent soft matrix because of its high stretchability and optical transparency, high thermal and environmental stability, as well as excellent mechanical strength.

Herein, we introduce a highly stretchable, skin-like temperature sensor by incorporating the thermochromic PDA into PDMS elastomer. The colorimetric signal upon thermal stimulus is easily recognized by the naked eyes. The stretchable capability is mainly from PDMS matrix, but highly enhanced by the involvement of PDA due to the enhanced crosslink density. The as-formed system demonstrates a stretchability up to 300%, with Young's modulus (~230 kPa) in the same range as skin. Given its simplicity and efficiency, the proposed system could serve as a rational guideline for design of a variety of wearable and disposable colorimetric sensor protocol. In particular, the skin-like property facilitates conformal adhesion to the skin and promises for noninvasive and convenient physical characterization of the epidermis.

EXPERIMENTAL SECTION

Preparation of PDA-embedded PDMS film

In a typical procedure, a dichloromethane solution (2 mL), containing 10,12-pentacosadiynoic acid (PCDA) (4 mg), was injected into the blend of PDMS elastomer base (2.0 g) and curing agent (10:1 wt. ratio). After removing dichloromethane in *vacuo*, the mixture was poured into a Petri dish and cured at room temperature for one day to get the half-cured PCDA film. The as-formed PCDA film was then irradiated (under mask) with a 254 nm UV lamp (1 mW cm^{-2}) for 2 min and cured for another day to give the blue-phase PDA film (denoted as PDA-T25). The film thickness was varied according to the added amount of the PDMS precursor, so it can be tuned just by changing the precursor amount. "USTB" mask was prepared by 3D printing.

Structural characterizations

The UV-visible absorption and transmittance spectra in the range of 400–800 nm were measured using UV−vis −NIR spectrophotometer (Cary 5000, Agilent Ltd.). The spectrophotometer was equipped with a heating and cooling stage (heating stage, Linkam PE120). Fluorescence spectra were recorded using an F-4500 fluorescence spectrophotometer. Raman spectra were recorded using a Renishaw Raman spectrometer (Invia reflex Raman microscope) equipped with a semiconductor-cooled CCD detector and a confocal Leica microscope. The spectrograph uses 1,800 g mm^{-1} gratings and a linearly polarized Nd:YAG laser (785 nm). The tensile strength of the PDA films was measured using a Universal Testing Machine (Testometric, UK) at a strain rate of 30 mm min^{-1} until break. A minimum of three measurements were taken for each sample. Here, PDA films were cut into dumbbell-shaped specimens with the size of 60 mm×8 mm, and clamped onto the fixtures with a same force for every test to minimize operator errors (Fig. S1).

RESULTS AND DISCUSSION

The skin consist of two layers, namely the epidermis (modulus, 140–600 kPa) and the dermis (modulus, 2–80 kPa) [32]. By comparison, PDMS has a tensile Young's modulus in the range of 1.32–2.97 MPa, slightly higher than that of skin [33–35]. It is proved that compatible component can endow the polymer blend improved mechanical properties [36]. The blend of PDMS and PDA might encourage a reduced Young's modulus. Meanwhile, as a commonly used transparent matrix, the transmittance of the as-prepared PDMS in our investigation was ~90% in the visible light region of 400–800 nm (Fig. S2), and thus assuring the color yield of PDA without interfering its normal light absorption. On the other hand, blue-colored PDA are prepared by in-

© Science China Press and Springer-Verlag GmbH Germany 2018

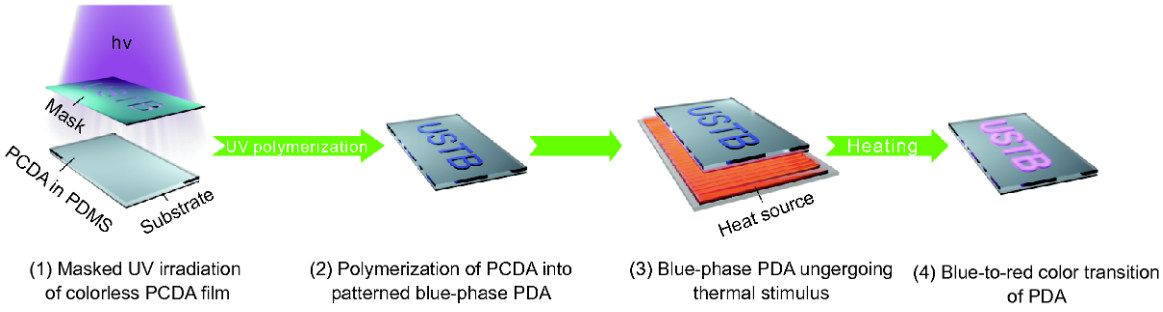

Figure 1 Schematic illustration of the design of the stretchable thermochromic temperature sensor.

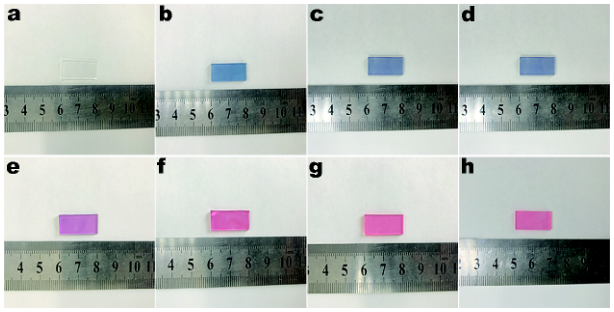

Figure 2 Photographs of pure PDMS film (a) and the polymerized PDA films at a heating temperature of 25, 40, 45, 50, 55, 60, and 70°C (b–h), denoted as PDA-25, PDA-40, PDA-45, PDA-50, PDA-55, PDA-60, and PDA-70, respectively according to the heating temperature.

itiator-free UV polymerization of self-assembled diacetylene monomers (colorless, Fig. S3). This advantage thus allows for one-step development of small-scale patterned functional images during UV polymerization, leading to the formation of patterned PDA embedded within the PDMS matrix for better color contrast or imaging. Based on these considerations, the strategy employed in this investigation was depicted in Fig. 1. (Masked) UV irradiation of the diacetylene monomer films generates (patterned) blue-colored images (Fig. S4). The as-obtained thin film could be rolled, twisted, bended, or stretched. It therefore can act as a wearable, or skin-mounted temperature sensor, which undergoes a blue-to-red color change or fluorescence change in response to thermal stimuli.

The visible change was firstly shown from the photographs of the blend film with regard to its thermochromic behavior (Fig. 2). Bare PDMS film was totally colorless and transparent (Fig. 2a). At room temperature, PDA-T25 was a typical blue-colored film (Fig. 2b) with a thickness of ~250 μm (Fig. S5). Cross section scanning electron microscopy (SEM) observation proved the good compatibility between PDA and PDMS in the blend, while negligible voids were observed and the two phases were hardly distinguishable (Fig. S6) [36]. The blue-colored film became purple at ~45°C (PDA-T45, Fig. 2d), and completely turned red near 55°C (PDA-T55, Fig. 2f). The apparent color transition can provide a visual signal for the temperature change.

To quantitatively evaluate the color transition of the PDA film, spectroscopic monitoring was conducted through the absorption and transmittance spectra over a broad temperature range of 25–100°C. As can be seen from Fig. S7a, the blue-phase PDA-T25 film shows a typical absorption spectrum with a maximum absorption peak at ~652 nm and another small one at ~595 nm. When heating from room temperature to 100°C, the maximum absorption shows a gradual decrease and blue shift, and finally converts into shorter wavelength with the absorption maximum near 545 nm characteristic of red-phase PDA. The maximum absorption shift ($\Delta\lambda_{652}$) as a function of temperature was plotted to gain insight into the thermochromic behavior (Fig. 3a). It could be observed that $\Delta\lambda_{652}$ displayed an upward tendency (25–70°C) until it reached a plateau. Previous reports usually used the colorimetric responses (%CR) to determine the temperature-dependent color transitions [28,29]. CR is referred to percentage change of the maximum absorption of the blue phase with respect to the total absorption of both red and blue phases. As a relative evaluation of the color transition, it is defined as $\%CR=100(PB_0-PB)/PB_0$, where $PB=A_{blue}/(A_{blue}+A_{red})$ and A is absorption. Fig. 3b shows the plot of %CR followed a sigmoidal curve upon increasing the temperature, and a sharp colorimetric transition was found to be within the range of 60–85°C. PDA film became increasingly transparent with rising temperature (Fig. S7b) and the integral luminous transmittance T_{lum} (400–800 nm) [37,38] was plotted in Fig. 3c and Fig. S7c. Based on %CR, sharp transmittance change was also observed to be within the range of 60–85°C. Here, T_{lum} provides a much easier way to measure the colorimetric transition than that of %CR. In addition

© Science China Press and Springer-Verlag GmbH Germany 2018

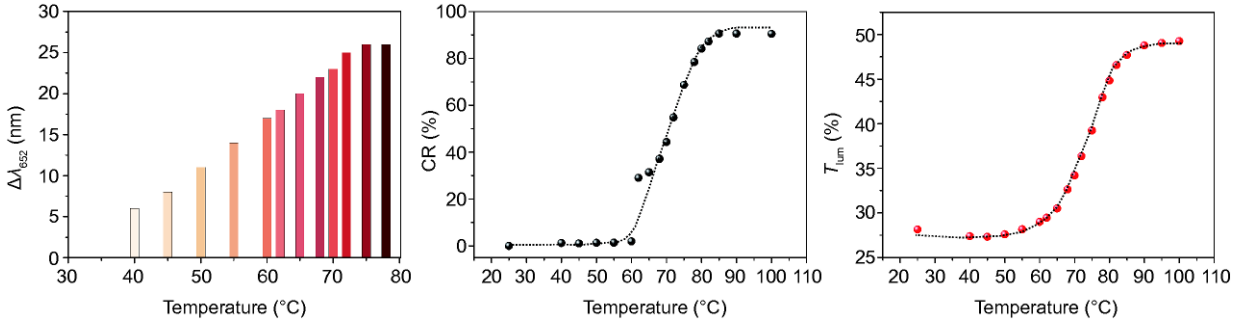

Figure 3 Plots of the maximum blue absorption shift $\Delta\lambda_{652}$ (a), the colorimetric responses %CR (b), and the integral luminous transmittance T_{lum} (400–800 nm) (c) as a function of temperature.

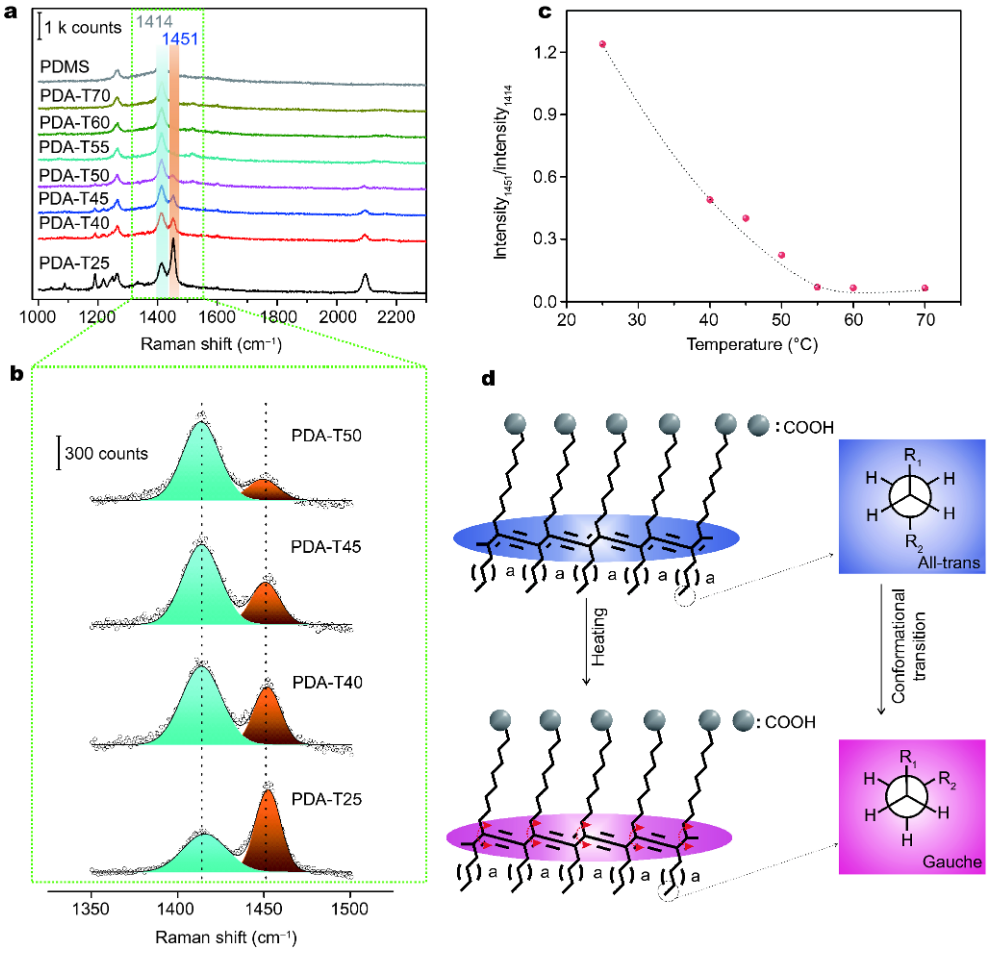

Figure 4 (a) Raman spectra of the as-prepared films; (b) magnified window of the green-dotted box in (a), showing PDMS (1414 cm^{-1}) and PDA (1451 cm^{-1}) fingerprints, which are used to calculate the temperature-dependent intensity ratio; (c) plots of Raman $intensity_{1451}/intensity_{1414}$ as a function of temperature; (d) proposed mechanism for the blue-to-red color transition. The applied heat induces the twist of backbone chain as well as single bond conformational change of a long alkyl side chain.

to the visual color transition, the fluorescence (Fig. S7d) induced by thermal stimuli is a useful tool to monitor the temperature change.

Changes in the molecular structure of PDA accounted for the color transition under thermal stimulus, as evidenced in Raman spectra (Fig. 4a). In 1,000–2,200 cm^{-1},

© Science China Press and Springer-Verlag GmbH Germany 2018

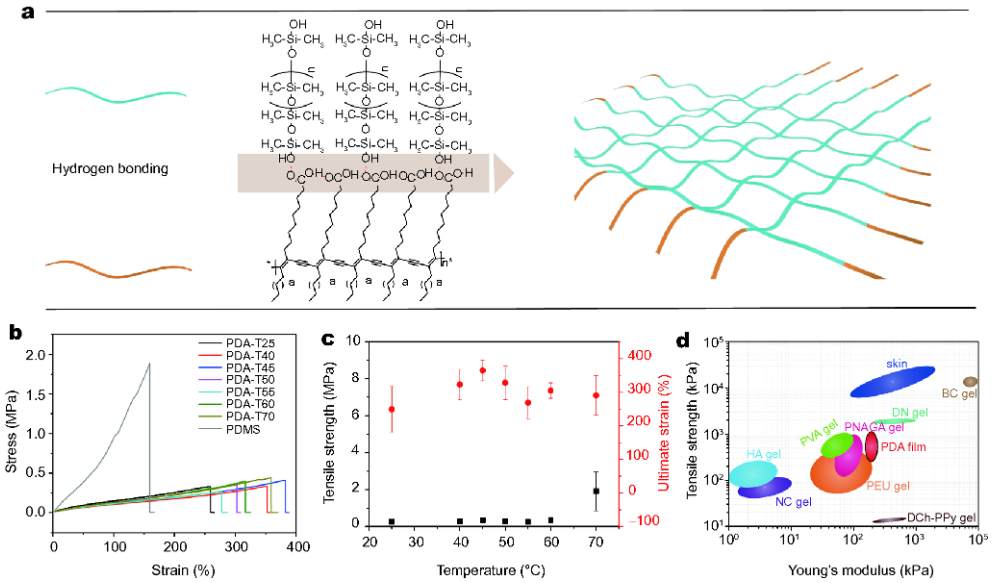

Figure 5 (a) Schematic representation of the physical crosslinking of PDMS and PDA; (b) tensile stress–strain curves of the as-prepared thin films; (c) plots of tensile strength and ultimate strain as a function of temperature; (d) tensile strength *versus* Young's modulus. Materials include the film prepared in this work (PDA film), polyvinyl alcohol gel (PVA gel) [41], double network gel (DN gel) [42], poly(*N*-acryloyl glycinamide) gel (PNAGA gel) [43], polyurethane (PEU gel) [44], polypyrrole-grafted chitosan gel (DCh-Ppy gel) [45], nanocomposite hydrogels (NC gel) [46], hydrophobic association hydrogels (HA gel) [47], bacterial cellulose gel (BC gel) [48] and skin [49–51].

PDMS showed two prominent bands at 1,414 cm^{-1} ($-CH_3$ asymmetric bend), and at 1,262 cm^{-1} ($-CH_3$ symmetric bend) [39]. As for the blue-phase PDA-T25, two bands associated with the conjugated alkene–alkyne structures were positioned at 2,095 cm^{-1} (C≡C vibration, $\nu_{C\equiv C}$) and 1,451 cm^{-1} (C=C vibration, $\nu_{C=C}$), respectively [28]. In addition, alkyl side chains of PDA gave rise to one strong band at 1,088 cm^{-1} and two weak bands at 1,104 and 1,129 cm^{-1}, and took fully extended all-trans C–C conformation [40]. The investigation of the fingerprint signals of each component during heating, namely 1,414 cm^{-1} for PDMS and 1,451 cm^{-1} for PDA in the 1,350–1,500 cm^{-1} window, revealed a gradual decrease of blue-phase PDA (Fig. 4b, c), which matched well with the absorbance and transmittance spectra. Along with the temperature increase, the $\nu_{C\equiv C}$ and $\nu_{C=C}$ of blue-phase PDA increased to 2,127 and 1,520 cm^{-1}, respectively, as shown in PDA-T55 (Fig. S8). This suggested a decrease of the conjugation length of the main chain. Meanwhile, the alkyl-related three bands of blue-phase PDA were replaced by one major band appearing at lower frequency (1,067 cm^{-1}), which suggested a probable alteration from the major all-trans conformation of the alkyl chain to gauche as temperature increased. Schematic illustration of such structural change was proposed in Fig. 4d. When the temperature elevated, the conjugated main chain of the PDA became twisted, and meantime a conformational variation in the side chains disrupted the π overlap and thus changed its planarity. These changes at last reduced the conjugation length and increased the energy band gap, hence leading to the change of the absorption wavelengths from 652 nm (blue phase) to 545 nm (red phase).

A skin-like sensor is required to display mechanical compliance as high as that of the human skin. Generally, the effective Young's moduli of the soft sensor is comparable to or lower than that of the epidermis thereby rendering conformal attachment onto or integration into the skin. Although PDMS matrix is not well-matched, PDA modifies the mechanical property by generating a high crosslink density because of the possible physical crosslinks. As schemed in Fig. 5a, the crosslinking of the PDMS was somewhat promoted by the formation of hydrogen bonds between the Si–OH end groups and the carboxyl group (–COOH) of the PDA [52]. The high crosslink density (the hydrogen bonding) thus enabled chain extension of PDMS and made the formed network more flexible and extensible. As evidenced in Fig. 5b, pure PDMS film possessed a tensile Young's modulus, ultimate tensile strength and elongation at break of ~1 MPa, 1.8 MPa and 150%, respectively. By comparison, the blue-phase PDA could sustain up to ~300% stretch-

 © Science China Press and Springer-Verlag GmbH Germany 2018

ing, and broke at a stress of ~250 kPa. More importantly, the presence of PDA brings about a reduction of the Young's modulus to ~230 kPa, a value that is quite compliant with human epidermis. The photographs of the film taken at different tensile strains could be seen in Fig. S9. Meanwhile, as temperature increased, PDA film maintained a relatively stable tensile strength and strain (Fig. 5c). Because the enhanced stretchability of PDMS-PDA film resulted from the high crosslink density (the hydrogen bonding) which was influenced greatly by temperature, a variation on the modulus of PDMS-PDA film was observed as temperature changed. In Fig. 5d, various transparent soft materials were compared in terms of their strength and elasticity [53]. Hydrogels constitute another type of transparent soft films [54–56]. However, different from the mechanically tough PDMS, the hydrogels are usually mechanically weak owing to their "wet" components (hygrophilic gel). As presented, PDA film performed much better than most hydrogel with respect to strength. Meanwhile, because of the enhanced elasticity, PDA film yields a Young's modulus in the same range of the skin.

CONCLUSIONS

In summary, we fabricated a disposable, skin-like thermochromic temperature sensor through physical crosslinking of transparent PDMS elastomer and thermochromic PDA. Thermal stimulus can initiate a perturbation in the arrangement of PDA molecules, and leads to a visual response. Absorption and transmittance spectroscopy determine the colorimetric transition. More importantly, physical crosslinking improves the mechanical property that is more compliant with the human skin. As a result, the as-prepared PDA film displays thermochromic transition temperature in the range of 25–85°C, with a Young's modulus of ~230 kPa that is comparable to that of human epidermis. To make it more applicable, the thermochromic transition temperature of a PDA polymer can be tuned to be closer to that of the human skin by modifying the PDA monomer. Overall, such soft blend film with directed response performance and skin-like elasticity may open up a rational guideline for developing novel functional materials and devices with desirable geometries and patterns.

Received 11 January 2018; accepted 28 March 2018; published online 16 April 2018

1 Lee H, Song C, Hong YS, *et al.* Wearable/disposable sweat-based glucose monitoring device with multistage transdermal drug delivery module. Sci Adv, 2017, 3: e1601314
2 Gao W, Emaminejad S, Nyein HYY, *et al.* Fully integrated wearable sensor arrays for multiplexed *in situ* perspiration analysis. Nature, 2016, 529: 509–514
3 Khan Y, Ostfeld AE, Lochner CM, *et al.* Monitoring of vital signs with flexible and wearable medical devices. Adv Mater, 2016, 28: 4373–4395
4 Jin H, Huynh TP, Haick H. Self-healable sensors based nanoparticles for detecting physiological markers *via* skin and breath: toward disease prevention via wearable devices. Nano Lett, 2016, 16: 4194–4202
5 Trung TQ, Lee NE. Flexible and stretchable physical sensor integrated platforms for wearable human-activity monitoringand personal healthcare. Adv Mater, 2016, 28: 4338–4372
6 Webb RC, Bonifas AP, Behnaz A, *et al.* Ultrathin conformal devices for precise and continuous thermal characterization of human skin. Nat Mater, 2013, 12: 938–944
7 Yan C, Kang W, Wang J, *et al.* Stretchable and wearable electrochromic devices. ACS Nano, 2013, 8: 316–322
8 Bao R, Wang C, Peng Z, *et al.* Light-emission enhancement in a flexible and size-controllable ZnO nanowire/organic light-emitting diode array by the piezotronic effect. ACS Photonics, 2017, 4: 1344–1349
9 Bao R, Wang C, Dong L, *et al.* CdS nanorods/organic hybrid LED array and the piezo-phototronic effect of the device for pressure mapping. Nanoscale, 2016, 8: 8078–8082
10 Xiang HY, Li YQ, Zhou L, *et al.* Outcoupling-enhanced flexible organic light-emitting diodes on ameliorated plastic substrate with built-in indium–tin-oxide-free transparent electrode. ACS Nano, 2015, 9: 7553–7562
11 Huang Y, Huang Y, Meng W, *et al.* Enhanced tolerance to stretch-induced performance degradation of stretchable MnO_2-based supercapacitors. ACS Appl Mater Interfaces, 2015, 7: 2569–2574
12 Chen S, Lou Z, Chen D, *et al.* Highly flexible strain sensor based on ZnO nanowires and P(VDF-TrFE) fibers for wearable electronic device. Sci China Mater, 2016, 59: 173–181
13 Zhang X, Zhang H, Lin Z, *et al.* Recent advances and challenges of stretchable supercapacitors based on carbon materials. Sci China Mater, 2016, 59: 475–494
14 Liu Z, Wang X, Qi D, *et al.* High-adhesion stretchable electrodes based on nanopile interlocking. Adv Mater, 2017, 29: 1603382
15 Qi D, Liu Z, Liu Y, *et al.* Highly stretchable, compliant, polymeric microelectrode arrays for *in vivo* electrophysiological interfacing. Adv Mater, 2017, 29: 1702800
16 Liu Z, Qi D, Hu G, *et al.* Surface strain redistribution on structured microfibers to enhance sensitivity of fiber-shaped stretchable strain sensors. Adv Mater, 2018, 30: 1704229
17 Hong SY, Lee YH, Park H, *et al.* Stretchable active matrix temperature sensor array of polyaniline nanofibers for electronic skin. Adv Mater, 2016, 28: 930–935
18 Trung TQ, Ramasundaram S, Hwang BU, *et al.* An all-elastomeric transparent and stretchable temperature sensor for body-attachable wearable electronics. Adv Mater, 2016, 28: 502–509
19 Chen Y, Lu B, Chen Y, *et al.* Breathable and stretchable temperature sensors inspired by skin. Sci Rep, 2015, 5: 11505
20 Yu C, Wang Z, Yu H, *et al.* A stretchable temperature sensor based on elastically buckled thin film devices on elastomeric substrates. Appl Phys Lett, 2009, 95: 141912
21 Dittmar A, Gehin C, Delhomme G, et al. In a non invasive wearable sensor for the measurement of brain temperature. Engineering in Medicine and Biology Society, 2006. EMBS'06. 28th

 © Science China Press and Springer-Verlag GmbH Germany 2018

Annual International Conference of the IEEE, 2006, 900–902
22 Jeon J, Lee HBR, Bao Z. Flexible wireless temperature sensors based on Ni microparticle-filled binary polymer composites. Adv Mater, 2013, 25: 850–855
23 Shih WP, Tsao LC, Lee CW, *et al.* Flexible temperature sensor array based on a graphite-polydimethylsiloxane composite. Sensors, 2010, 10: 3597–3610
24 Lan M, Liu W, Ge J, *et al.* A selective fluorescent and colorimetric dual-responses chemosensor for streptomycin based on polythiophene derivative. Spectrochim Acta Part A-Mol Biomol Spectr, 2015, 136: 871–874
25 Xu Y, Wu X, Chen Y, *et al.* Fiber-optic detection of nitroaromatic explosives with solution-processable triazatruxene-based hyperbranched conjugated polymer nanoparticles. Polym Chem, 2016, 7: 4542–4548
26 Xu Y, Wu X, Chen Y, *et al.* Star-shaped triazatruxene derivatives for rapid fluorescence fiber-optic detection of nitroaromatic explosive vapors. RSC Adv, 2016, 6: 31915–31918
27 Ahn DJ, Chae EH, Lee GS, *et al.* Colorimetric reversibility of polydiacetylene supramolecules having enhanced hydrogen-bonding under thermal and pH stimuli. J Am Chem Soc, 2003, 125: 8976–8977
28 Park IS, Park HJ, Jeong W, *et al.* Low temperature thermochromic polydiacetylenes: design, colorimetric properties, and nanofiber formation. Macromolecules, 2016, 49: 1270–1278
29 Dong W, Lin G, Wang H, *et al.* New dendritic polydiacetylene sensor with good reversible thermochromic ability in aqueous solution and solid film. ACS Appl Mater Interfaces, 2017, 9: 11918–11923
30 Lee J, Yarimaga O, Lee CH, *et al.* Network polydiacetylene films: preparation, patterning, and sensor applications. Adv Funct Mater, 2011, 21: 1032–1039
31 Yoon B, Ham DY, Yarimaga O, *et al.* Inkjet printing of conjugated polymer precursors on paper substrates for colorimetric sensing and flexible electrothermochromic display. Adv Mater, 2011, 23: 5492–5497
32 Kim DH, Lu N, Ma R, *et al.* Epidermal electronics. Science, 2011, 333: 838–843
33 Liu M, Sun J, Sun Y, *et al.* Thickness-dependent mechanical properties of polydimethylsiloxane membranes. J Micromech Microeng, 2009, 19: 035028
34 Brown XQ, Ookawa K, Wong JY. Evaluation of polydimethylsiloxane scaffolds with physiologically-relevant elastic moduli: interplay of substrate mechanics and surface chemistry effects on vascular smooth muscle cell response. Biomaterials, 2005, 26: 3123–3129
35 Johnston ID, McCluskey DK, Tan CKL, *et al.* Mechanical characterization of bulk Sylgard 184 for microfluidics and microengineering. J Micromech Microeng, 2014, 24: 035017
36 Mistretta MC, Ceraulo M, La Mantia FP, *et al.* Compatibilization of polyethylene/polyamide 6 blend nanocomposite films. Polym Compos, 2015, 36: 992–998
37 Ke Y, Wen X, Zhao D, *et al.* Controllable fabrication of two-dimensional patterned VO_2 nanoparticle, nanodome, and nanonet arrays with tunable temperature-dependent localized surface plasmon resonance. ACS Nano, 2017, 11: 7542–7551
38 Ke Y, Balin I, Wang N, *et al.* Two-dimensional SiO_2/VO_2 photonic crystals with statically visible and dynamically infrared modulated for smart window deployment. ACS Appl Mater Interfaces, 2016, 8: 33112–33120
39 Cai D, Neyer A, Kuckuk R, *et al.* Raman, mid-infrared, near-infrared and ultraviolet–visible spectroscopy of PDMS silicone rubber for characterization of polymer optical waveguide materials. J Mol Structure, 2010, 976: 274–281
40 Lippert JL, Peticolas WL. Laser raman investigation of the effect of cholesterol on conformational changes in dipalmitoyl lecithin multilayers. Proc Natl Acad Sci USA, 1971, 68: 1572–1576
41 Zhang L, Zhao J, Zhu J, *et al.* Anisotropic tough poly(vinyl alcohol) hydrogels. Soft Matter, 2012, 8: 10439–10447
42 Yin H, Akasaki T, Lin Sun T, *et al.* Double network hydrogels from polyzwitterions: high mechanical strength and excellent anti-biofouling properties. J Mater Chem B, 2013, 1: 3685–3693
43 Dai X, Zhang Y, Gao L, *et al.* A mechanically strong, highly stable, thermoplastic, and self-healable supramolecular polymer hydrogel. Adv Mater, 2015, 27: 3566–3571
44 Frydrych M, Román S, Green NH, *et al.* Thermoresponsive, stretchable, biodegradable and biocompatible poly(glycerol sebacate)-based polyurethane hydrogels. Polym Chem, 2015, 6: 7974–7987
45 Darabi MA, Khosrozadeh A, Mbeleck R, *et al.* Skin-inspired multifunctional autonomic-intrinsic conductive self-healing hydrogels with pressure sensitivity, stretchability, and 3D printability. Adv Mater, 2017, 29: 1700533
46 Haraguchi K, Takehisa T. Nanocomposite hydrogels: a unique organic–inorganic network structure with extraordinary mechanical, optical, and swelling/de-swelling properties. Adv Mater, 2002, 14: 1120–1124
47 Jiang G, Liu C, Liu X, *et al.* Network structure and compositional effects on tensile mechanical properties of hydrophobic association hydrogels with high mechanical strength. Polymer, 2010, 51: 1507–1515
48 Svensson A, Nicklasson E, Harrah T, *et al.* Bacterial cellulose as a potential scaffold for tissue engineering of cartilage. Biomaterials, 2005, 26: 419–431
49 Diridollou S, Patat F, Gens F, *et al. In vivo* model of the mechanical properties of the human skin under suction. Skin Res Technol, 2000, 6: 214–221
50 Daly CH. Biomechanical properties of dermis. J Invest Dermatology, 1982, 79: 17–20
51 Ní Annaidh A, Bruyère K, Destrade M, *et al.* Characterization of the anisotropic mechanical properties of excised human skin. J Mech Behav BioMed Mater, 2012, 5: 139–148
52 Tugui C, Vlad S, Iacob M, *et al.* Interpenetrating poly(urethane-urea)–polydimethylsiloxane networks designed as active elements in electromechanical transducers. Polym Chem, 2016, 7: 2709–2719
53 Li J, Suo Z, Vlassak JJ. Stiff, strong, and tough hydrogels with good chemical stability. J Mater Chem B, 2014, 2: 6708–6713
54 Keplinger C, Sun JY, Foo CC, *et al.* Stretchable, transparent, ionic conductors. Science, 2013, 341: 984–987
55 Hao GP, Hippauf F, Oschatz M, *et al.* Stretchable and semitransparent conductive hybrid hydrogels for flexible supercapacitors. ACS Nano, 2014, 8: 7138–7146
56 Cipriano BH, Banik SJ, Sharma R, *et al.* Superabsorbent hydrogels that are robust and highly stretchable. Macromolecules, 2014, 47: 4445–4452

Acknowledgements This work was supported by the National Key Research and Development Program of China (2016YFB0700300), the National Natural Science Foundation of China (51503014 and

 © Science China Press and Springer-Verlag GmbH Germany 2018

51501008), and the State Key Laboratory for Advanced Metals and Materials (2016Z-03).

Author contributions Chen Y designed and engineered the samples; Xi Y performed the experiments with support from Ke Y; Chen Y wrote the paper. All authors contributed to the general discussion.

Conflict of interest The authors declare no conflict of interest.

Supplementary information Additional characterizations are available in the online version of the paper.

Yingzhi Chen is a Lecturer of the School of Materials Science and Engineering, University of Science and Technology Beijing, China. Her research mainly focuses on the design, fabrication of optoelectronic compounds & devices, as well as novel biomedical materials.

Lu-Ning Wang is a Thousand Youth Talent, Professor and Dean of the School of Materials Science and Engineering, University of Science and Technology Beijing, China. His research mainly focuses on the design, preparation, theoretical study of novel biomedical materials. He has published more than 20 peer reviewed papers, and is an editorial board member of *International Journal of Nanomedicine*.

Xiaohong Zhang is a Chang Jiang Scholar, Professor and Vice President of Soochow University. His research interests include organic optoelectronic materials, semiconductor nanomaterials, and optoelectronic devices. He has published more than 200 peer reviewed papers and applied more than 40 patents.

皮肤式可拉伸变色温度传感器

陈颖芝[1], 席鉴[1], 柯宇杰[2], 李文昊[1], 龙祎[2], 李静媛[1], 王鲁宁[1,3*], 张晓宏[4*]

摘要 可穿戴传感器最主要的形式为直接与皮肤接触式, 用于测量各种皮肤表面参数. 一种创新型的传感器使用柔软和极端轻薄的材料, 其机械性质和延展性与人体表皮相似, 因此也被称为表皮传感器. 表皮传感器能够自发地附着在皮肤上, 顺应皮肤的表面形态. 本论文利用PCDA聚合后的热致变色特性, 及PDMS高分子基体良好的拉伸性, 通过物理交联的方法, 制备了可拉伸的柔性热致变色温度传感器. 对PDA/PDMS薄膜进行热致变色及力学性能探究发现 PDA薄膜具有较低的变色温度区间25–85°C, 其断裂延伸率平均可达300%, 杨氏模量接近表皮约为230 kPa. 该方法为发展生物相容性传感体系提供了良好的理论与实际参考.

 © Science China Press and Springer-Verlag GmbH Germany 2018